Near Infrared (NIR) lanthanide emissive Langmuir-Blodgett monolayers formed using Nd(III) directed self-assembly synthesis of chiral amphiphilic ligands

Dawn E. Barry[†], *Jonathan A. Kitchen*[*†], *Martin Albrecht*[‡], *Stephen Faulkner*[§], *and Thorfinnur Gunnlaugsson*[*,†]

[†]School of Chemistry and Trinity Biomedical Science Institute, Trinity College Dublin, Dublin 2, Ireland. [‡]School of Chemistry and Chemical Biology, University College Dublin, Belfield, Dublin 4, Ireland. [§]University of Oxford, Chemistry Research Laboratories, 12 Mansfield Road, Oxford OX1 3TA. U.K.

gunnlaut@tcd.ie, j.a.kitchen@soton.ac.uk

KEYWORDS: Langmuir, Langmuir-Blodgett, lanthanide luminescence, NIR emission, self-assembly, monolayers, chirality

The incorporation of chiral amphiphilic lanthanide-directed self-assembled Nd^{III} complexes (**Nd.1**$_3$ and **Nd.2**$_3$) into stable Langmuir monolayers, and the subsequent Langmuir-Blodgett film formation of these, is described. The photophysical properties of the enantiomeric pair of ligands **1** and **2** in the presence of $Nd(CF_3SO_3)_3$ were also investigated in CH_3CN solutions using UV-Vis, fluorescence, lanthanide luminescence spectroscopies. Analysis of the resulting self-assembly processes revealed that two main species were formed in solution – 1:1 and 1:3 **Nd:L**

self-assembly complexes; with the latter being the dominant species upon the addition of 0.33 equivalents of Nd^{III}. Excited state lifetime measurements of **Nd.1$_3$** and **Nd.2$_3$** in CH_3OH and CD_3OD and CH_3CN were also evaluated. Surface pressure-area and surface pressure-time isotherms evidenced the formation of stable Langmuir monolayers of **Nd.1$_3$** and **Nd.2$_3$** at an air-water interface, and the deposition of these monolayers onto a quartz solid substrate (Langmuir-Blodgett films) gave rise to immobilized chiral monomolecular films which exhibited Nd^{III} NIR luminescence.

Introduction

The development of functional nano-structures using lanthanide-directed self-assembly has been a growing area of interest in recent times; as such systems have potential applications, in molecular recognition/sensing, imaging and for use in optical devices.[1,2,3-6] The lanthanides, both visibly emitting (Eu^{III}, Tb^{III} and Sm^{III}) and NIR emitting (Nd^{III} and Yb^{III}), are ideal candidates for such applications as they possess long lived excited states and well defined narrow line-like emission bands.[3,7-9] However, the transitions are spin forbidden and generation of the excited states is best achieved through the use of a sensitizing chromophore (the antenna effect).[9] The NIR emitting lanthanides, such as Pr^{III}, Yb^{III}, Er^{III} and Nd^{III}, offer major advantages over other visibly emitting lanthanides for applications in biology,[10] such as in the development of luminescent imaging agents and bioprobes, as the NIR emission (800 – 1000 nm) is transparent to biological tissue, therefore allowing imaging through relatively thick tissue samples. Moreover, from an optical devices point of view, the NIR emissive lanthanides can be employed in telecommunications optical networks, again owing to their emission in the transparent window of silica fibers (1000 – 1600 nm). [11] Of the NIR emitting lanthanides, Nd^{III} and Er^{III} are particularly interesting as the luminescent behavior is highly sensitive to the external

environment.[12-15] In particular, the high density of states in the excited state manifolds of Nd^{III} and Er^{III} ensures that non-radiative quenching of the lanthanide emissive state by associated C-H and O-H oscillators is more important in complexes with these ions than any other lanthanides, as they are quenched to a greater extent through closely associated C-H oscillators (in addition to N-H and O-H oscillators).[2,12,15-17] As well as introducing a strong dependence of luminescence quantum yield and lifetime upon structure, this phenomenon also means that ternary assemblies, involving guests such as biomolecules and complexes, will change the luminescence quantum yields of such species.[18-20] Such assemblies have already been widely exploited in systems where inner sphere solvation is changed when the assembly is formed;[21,22] however, there is also clear potential to exploit the more subtle effects inherent to the presence of local oscillators in lifetime resolved imaging. For practical application, Nd^{III} complexes are ideal as luminescence quantum yields from Er^{III} complexes in aqueous media tend to be very low indeed as a consequence of the small energy gap between the emissive state and ground state.

Often practical applications for luminescent lanthanide complexes/self-assemblies require their immobilization onto solid supports. However, not only must the Ln^{III} be incorporated into/onto the solid support, but the desirable features of the Ln^{III} system must be retained, i.e. surface attachment should not significantly alter the attractive luminescent properties observed in the bulk solid or in solution. To this end, significant research has been ongoing to incorporate luminescent complexes into solid supports. Our own efforts have resulted in the development of luminescent lanthanide systems within hydrogels[23,24] or conjugated to the surface of gold nanoparticles,[25-27] where in all cases there is retention of Ln^{III} luminescent characteristics on transfer from solution to solid.[28] Furthermore, recently we have also shown that chiral Eu^{III} based complexes can be transferred to the surface of quartz solid substrates by utilizing the Langmuir-

Blodgett technique, and the retention of photophysical properties is again observed, including retention of circularly polarized luminescence (CPL).[28] With the view of extending out interest in the development of functional lanthanide luminescent structures, we set out to form highly organized Langmuir monolayers formed by using lanthanide directed self-assembly from NIR emitting lanthanides. Furthermore, our objective was to then transfer these monolayers onto solid supports, giving rise to new surface bound materials with additional advantages over other solid matrix immobilization techniques currently being employed such as deposition precision, order and control. Herein we detail the results from this study, carried out using the chiral ligands **1** and **2** (Scheme 1) and Nd^{III}. Investigation into the ability of these complexes to form luminescent self-assemblies as well as their ability to give stable Langmuir monolayers at an air-water interface was undertaken. Following deposition and subsequent Langmuir-Blodgett film formation, the photophysical properties of the immobilized monolayers of **Nd.1$_3$** and **Nd.2$_3$** were also investigated in detail, and to the best of our knowledge, these are the first examples of such lanthanide NIR emitting self-assembled monolayers to be developed to date.

Experimental Section

General All starting materials were purchased from commercial sources and used as received. Solvents were of HPLC grade and used without purification. Electro mass spectra was determined using a Mass Lynx NT V 3.4 on a Waters 600 controller connected to a 996 photodiode array detector with HPLC-grade CH_3CN, CH_2Cl_2 or CH_3OH as carrier solvents. A peak-matching method was used to determine accurate molecular weights using leucine enkephaline (H-Tyr-Gly-Gly-Phe-Leu-OH) as the standard reference (m/z = 556.2771); all accurate mass were reported within ± 5 ppm of the expected mass. Elemental analyses were

carried out at the Microanalytical Laboratory, School of Chemistry and Chemical Biology, University College Dublin. Infrared spectra were recorded on a Perkin Elmer Spectrum One FT-IR spectrometer equipped with a Universal ATR sampling accessory. Solid samples were recorded directly as neat samples in cm^{-1}. Complexation reactions were carried out in 2-5 mL Biotage Microwave Vials in a Biotage Initiator Eight EXP microwave reactor. Reactions were performed at 70 °C for 10 minutes in HPLC grade methanol. Single crystal X-ray diffraction data for **1** were collected using graphite monochromated Cu Kα radiation (λ = 1.54184 Å) on an Oxford Diffraction SuperNova diffractometer. The diffractometer was equipped with a Cryostream N_2 open-flow cooling device,[29] and the data were collected at 150(2) K. Series of ω-scans were performed in such a way as to collect all unique reflections to a maximum of 0.80 Å. Cell parameters and intensity data (including inter-frame scaling) were processed using CrysAlis Pro.[30] The structure was solved by direct methods (SHELXS-97) and refined against all F^2 data (SHELXL-97).[31] Non-hydrogen atoms were refined with anisotropic displacement parameters. Hydrogen atoms, except for N-H protons, were positioned geometrically and refined using a riding model with d(CH_{aro}) =0.95 Å, *U*iso = 1.2*U*eq (C) for aromatic, d(CH) =1.0 Å, *U*iso = 1.2*U*eq (C) for CH, 0.99 Å, *U*iso = 1.2*U*eq (C) for CH_2 and 0.98 Å, *U*iso = 1.2*U*eq (C) for CH_3. Amide N-H protons were found from the difference map and fixed to the attached atoms.

Synthesis: Complexes **Nd.1$_3$** and **Nd.2$_3$** were prepared by the reaction of **1** or **2** (30 mg, 0.06 mmol) in 5 mL CH_3OH which had solid $Nd(CF_3SO_3)_3$ (18 mg, 0.03 mmol) added and was heated at 70 °C under microwave irradiation for 10 minutes. The resulting clear yellow solutions were subjected to vapour diffusion of diethyl ether resulting in the formation of solids.

$[Nd(1)_3](CF_3SO_3)_3$ ($Nd.1_3$): Formed as white solid, 22 mg (50%). Elemental analysis for $C_{108}H_{147}N_9O_{15}F_9S_3Nd.3H_2O$ calc: C 56.97, H 6.77, N 5.54; found C 56.57, H 6.25, N 5.66%. IR(neat): 3290, 2920, 2853, 1631 (C=O), 1594, 1560, 1458, 1238, 1164, 1030, 800, 779, 753 cm^{-1}. HR-MALDI-MS: 1526.5824 ($[M\text{-}L\text{-}CF_3SO_3]^+$, $C_{72}H_{98}N_6O_{10}F_6S_2Nd^+$; calc 1526.5767).

$[Nd(2)_3](CF_3SO_3)_3$ ($Nd.2_3$): Formed as white solid, 26 mg (59%). Elemental analysis for $C_{108}H_{147}N_9O_{15}F_9S_3Nd$ (2218.91 $gmol^{-1}$) calc: C 58.41, H 6.68, N 5.68; found C 58.94, H 6.67, N 5.74%. IR(neat): 3292, 2925, 2854, 1633 (C=O), 1594, 1559, 1457, 1237, 1165, 1030, 800, 778, 752 cm^{-1}. HR-MALDI-MS: 1526.5822 ($[M\text{-}L\text{-}CF_3SO_3]^+$, $C_{72}H_{98}N_6O_{10}F_6S_2Nd^+$; calc. 1526.5767).

Photophysical studies: The UV-visible absorption spectra were recorded at RT using a Varian Cary 50-spectrophotometer. The solvent employed was of HPLC grade. The wavelength range was set from 450 nm to 200 nm with a scan rate of 600 nm min^{-1}. Circular dichroism (CD) spectra were recorded on a Jasco J-810-150S spectropolarimeter. Luminescence spectra in the near-IR region was recorded on a Fluorolog FL 3-22 spectrophotometer from Horiba-Jobin-Yvon with double grating emission and excitation monochromators, and a R5509-73 photomultiplier. Light intensity was measured by a C9940-22 detector from Hamamatsu (range 800-1700 nm) cooled to 77 K and coupled to a Jobin Yvon SpectrAcq v5.20 data acquisition system. For the measurement of the Nd^{III} luminescence lifetimes, the samples were excited using a pulsed nitrogen laser (PTI-3301, 337 nm) operating at 10 Hz. Light emitted at right angles to the excitation beam was focused onto the slits of a monochromator (PTI120), which was used to select the appropriate wavelength. The growth and decay of the luminescence at selected wavelengths were detected using a germanium photodiode (Edinburgh instruments, EI-P) and recorded using a digital oscilloscope (Tektronix TDS220) before being transferred to a PC for

analysis. Time-resolved emission spectra were obtained by measuring the growth and decay of the luminescence at each of a series of wavelengths. Luminescence lifetimes were obtained by iterative reconvulution of the detector response (obtained using a scatterer) with exponential components for growth and decay of the metal centered luminescence, using a spreadsheet running in Microsoft Excel. The details of this approach have already been discussed.[12]

Langmuir film measurements: Surface-pressure isotherms and time stability were measured at 25 ºC on a KSV MiniMicro Langmuir-Blodgett trough (KSV, Finland) with a surface area between 1700 and 8700 mm^2. Water was purified with a Milli-Q® Integral system (Millipore), and its resistivity was measured to be higher than 18 MΩ cm. A 9:1 mixture of $CHCl_3$:CH_3OH was used as spreading solvent for complexes Nd.$\mathbf{1}_3$ and Nd.$\mathbf{2}_3$. Typically drops (20 μL) of the surfactant solution (~2.4 x 10^{-4} M) were deposited using a microsyringe on the water subphase. After leaving to evaporate for 20 minutes, the barriers were compressed at 6 mm min^{-1} and the surface pressure was monitored using a platinium Wilhelmy plate. Quartz slides for dipping experiments were immersed in conc. HNO_3 (30 minutes), piranha solution (3:1 H_2SO_4:H_2O_2) (30 minutes) and rinsed well with de-ionized water immediately prior to use.

Results and Discussion

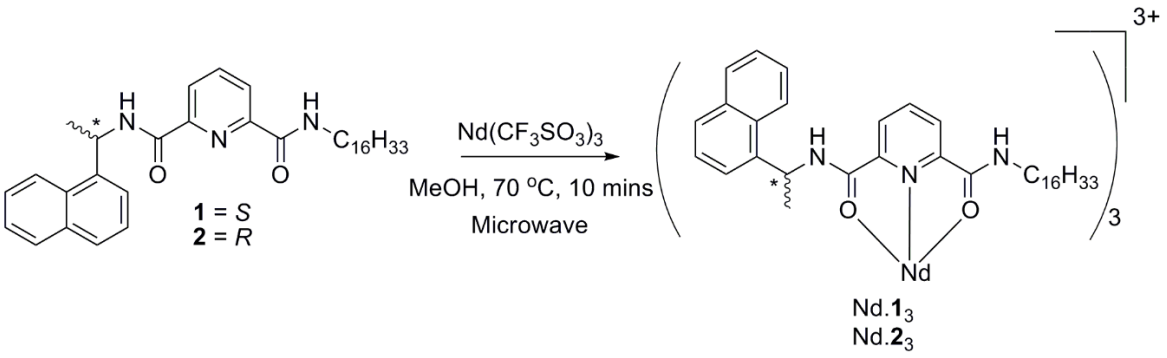

Scheme 1. Complexation of ligands **1** and **2** with $Nd(CF_3SO_3)_3$ affording the desired **Nd.1$_3$** and **Nd.2$_3$** complexes.

Synthesis and characterization: Ligands **1** and **2** were prepared according to our previously reported procedure, as shown in Scheme 1.[28] In addition colorless, X-ray quality rod shaped single crystals of **1** were obtained from the slow evaporation of a CH_3CN/CH_2Cl_2 solution and the low temperature (123 K) structure determined. **1** crystallized in the chiral, monoclinic space group, $P2_1$, and contained two crystallographically independent molecules in the asymmetric unit as shown in Figure 1 (See also Supporting Information) and Table 1. The two independent molecules differ in the conformation of the hexadecyl chain. In one molecule the chain is relatively *trans* co-planar, (straight chain) whilst in the second molecule the chain has a twisted orientation as shown in Figure 1. The two molecules interact through NH···O hydrogen bonding, (see Table 1), and offset face to face π···π stacking between the pyridyl ring of one molecule and the naphthalene ring of the other (Figure 1). The crystal structure of **2** is isomorphous to that of **1** albeit of the other isomer.

The complexes **Nd.1$_3$** and **Nd.2$_3$** ($[Nd(\mathbf{L})_3](CF_3SO_3)_3$) were prepared from **1** and **2**, respectively, by reacting with $Nd(CF_3SO_3)_3$ in 3:1 stoichiometry in CH_3OH for 10 minutes under microwave irradiation. The pale yellow solutions were then subjected to vapor diffusion of diethyl ether yielding white solids in 50% and 59% yields, respectively. Elemental analysis

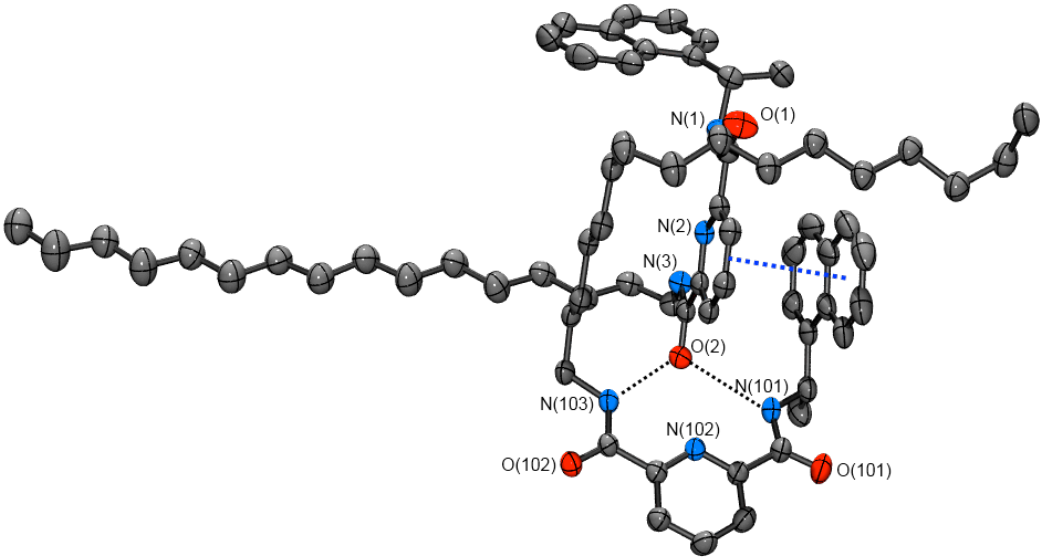

Figure 1. Perspective view of ligand **1** with thermal ellipsoids shown at 50% probability, illustrating dimeric nature of packing – note that π-π stacking (····) [centroid···centroid = 3.65 Å] and hydrogen bonding (····) [see Table 1] exists between the two crystalloraphically independent molecules. Hydrogen atoms have been omitted for clarity.

confirmed the formation of the desired products **Nd.1**$_3$ and **Nd.2**$_3$, whereas ESMS gave dominantly the *m/z* for the formation of the 1:2 complex formations **Nd.1**$_2$ and **Nd.2**$_2$.

Table 1. Hydrogen bonds for 1 [Å and °].

D-H...A	d(D-H)	d(H...A)	d(D...A)	<(DHA)
N(1)-H(1X)...O(102)[a]	0.89	2.19	3.0500(18)	162.0
N(3)-H(3X)...O(102)[a]	0.87	2.12	2.9447(18)	158.3
N(101)-H(10X)...O(2)[b]	0.9	2.18	3.0192(18)	154.9
N(103)-H(10Y)...O(2)[b]	0.9	2.15	3.0105(17)	158.2

Photophysical characterization of Nd.1$_3$ and Nd.2$_3$

The photophysical properties of **Nd.1**$_3$ and **Nd.2**$_3$ were first evaluated in CH_3CN and CH_3OH solutions (See supporting informations Figures S1-S6). The UV-Visible absorption spectra of

these complexes were dominated by an absorption assigned to the naphthalene antenna $\pi \rightarrow \pi^*$ with $\square_{max}$ = 281 nm, and by the n $\rightarrow \pi^*$ transition of the central pyridyl unit at $\square_{max}$ = 223 nm, with the long wavelength band tailing to ca. 350 nm. Excitation of the naphthalene antennae at 281 nm gave rise on both occasions to Nd^{III} centered luminescence indicating effective sensitization of the $^4F_{3/2}$ excited state and subsequent deactivation to the ^4I_J (J = 9/2, 11/2, 13/2) states with line-like emission bands observed at 880 nm ($^4F_{3/2} \rightarrow {}^4I_{9/2}$), 1064 nm ($^4F_{3/2} \rightarrow {}^4I_{11/2}$) and 1334 nm ($^4F_{3/2} \rightarrow {}^4I_{13/2}$). Time resolved emission spectra (TRES) were also recorded for both **Nd.1$_3$** and **Nd.2$_3$** in CH_3CN as shown in Figure 2, and supporting information Figure S7. The Nd^{III}

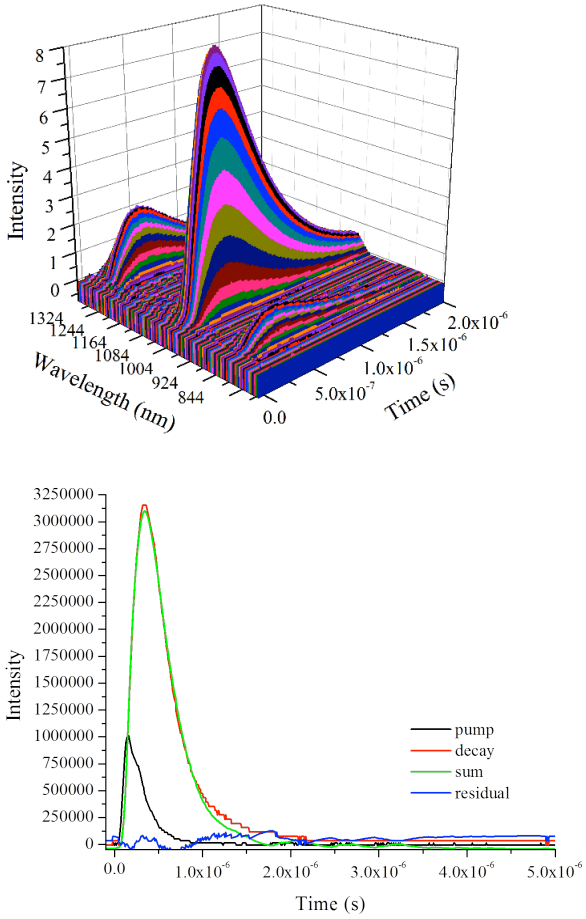

Figure 2. Top: Time-resolved emission spectrum of **Nd.1$_3$** after excitation at 337 nm, showing sensitized lanthanide-based luminescence. Bottom: Decay curve obtained from Nd.**1**$_3$ in CH_3OH and residuals for fitted curve generated by deconvulution of the instrument response function with a single exponential function.

luminescence decays (excitation at 337 nm) of the three transitions 880 nm ($^4F_{3/2}\rightarrow{}^4I_{9/2}$), 1064 nm ($^4F_{3/2}\rightarrow{}^4I_{11/2}$) and 1334 nm ($^4F_{3/2}\rightarrow{}^4I_{13/2}$) were observed. Lifetime measurements at 1064 nm fitted well to a model in which the data was fitted to components for rise time and decay by

Table 2. The Nd^{III} centered lifetimes (τ/ns) for $Nd(^4F_{3/2})$ in **Nd.1$_3$** and **Nd.2$_3$** as measured in in CH_3OH, CD_3OD and CH_3CN, respectively. Each measurement is an average of three independent measurements.

	MeOH		CD_3OD		MeCN	
	$\tau_{\text{rise time}}$ (ns)	τ (ns)	$\tau_{\text{rise time}}$ (ns)	τ (ns)	$\tau_{\text{rise time}}$ (ns)	τ (ns)
Nd.**1**$_3$	16	206	45	775		
Nd.**2**$_3$	12	251	40	865		

reconvolution with the detector response. Similar behavior was observed when measurements were conducted in CH_3OH and CD_3OD, as can be seen from the data in Table 2 and the typical fitted temporal profile shown in Figure 2. The rise-time in such systems generally arises from involvement of the triplet state of the donor chromophore in energy transfer to the lanthanide. This is borne out in these data by the differences observed between the rise time in CH_3OH and that in CD_3OD: longer rise times in deuterated media reflect the imperfect overlap between the triplet state of the donor chromophore and phonon assistance involving the solvent vibrational manifold, and the lower energy (and less effective spectral overlap) of C-D and O-D vibrational oscillators relative to analogous C-H and O-H oscillators. It is clear from the data in Table 2 that both Nd^{III} containing systems exhibit similar luminescence lifetimes in each of the solvent systems studied.

Due to the profound dependence of the luminescence lifetime of Nd^{III} complexes upon ligand structure it is unwise to use the published equations which were established for aminocarboxylate ligand systems derived from cyclen, to calculate the number of inner sphere

water molecules (q).[12,15] However, the lifetimes are consistent with a low degree of solvation at the metal center- those in CH_3OH are very long for a Nd^{III} complex. If we accept that the NO_2 donor sets of the three dipicolinamide ligands fill the inner coordination sphere, the differences between the values for the decay components of the luminescence lifetimes obtained in CH_3OH and CD_3OD are highly instructive. Clearly, two complexes do not constitute a sufficient body of data to establish meaningful relations that define q in dipicolinate systems, but it may be useful to consider an equation of the form:

$$q = A(1/\tau_{CH_3OH} \text{ and } 1/\tau_{CD_3OD} - B)$$

In a system in which there is no coordinated solvent, the difference between $1/\tau_{CH3OH}$ and $1/\tau_{CD3OD}$ should reflect B, the outer sphere solvent contribution to non-radiative deactivation of the excited state. On this basis, **Nd.1$_3$** and **Nd.2$_3$** give values of 3.5±0.6 μs^{-1} and 2.8±0.5 μs^{-1} respectively. These values are within error of one another and imply that the coordination environments and the nature of the solvation of the two complexes are very similar. It also differs significantly from the value of this outer sphere correction obtained for aminocarboxylate ligand systems (1.4 μs^{-1}),[15] suggesting that there may be significant variations in outer sphere solvent effects between different classes of complex.

Circular Dichroism (CD) studies of 1 and 2 with Nd(CF$_3$SO$_3$)$_3$: Circular dichroism spectra were recorded for **1** and **2**, as well as the Nd(III) complexes **Nd.1$_3$** and **Nd.2$_3$** in CH_3CN, the latter being formed in solution upon addition of 0.33 equivalents of Nd(III). The ligand CD demonstrated that **1** and **2** are formed as enantiomers; where mirror-image CD were observed, which is consistent with the presence of a single chiral stereoisomer in solution for these two ligands. For ligand **1** (the *S*-enantiomer) positive CD-bands appeared at 206, 229 and 287 nm and

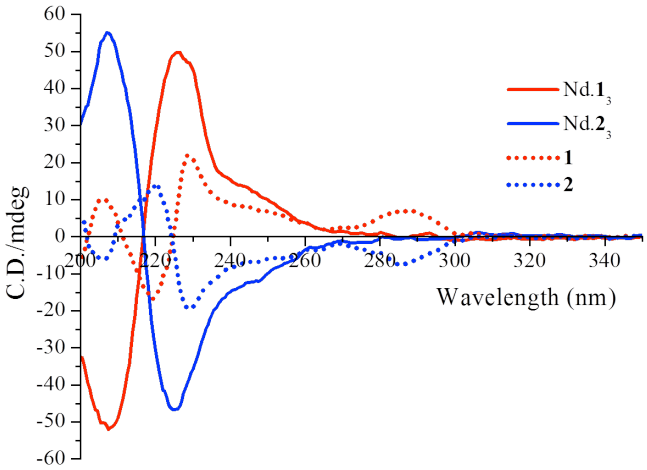

Figure 3. Circular dichroism spectra of ligands **1** and **2** and complexes **Nd.1$_3$** and **Nd.2$_3$**.

a broad shoulder at 250 nm, and a negative CD-band at 218 nm. The *R* isomer **2**, gave the exact opposite signals at these same wavelengths, Figure 3. Equal but opposite dichroism bands were also observed in the CD spectrum of the two complexes **Nd.1$_3$** and **Nd.2$_3$**. However, these were structurally different to that seen for their corresponding ligands; as in the case of **Nd.1$_3$** as only two main bands were observed, a negative band at 207 nm and a positive band centered at 224 nm, respectively. However as before, a positive broad band also occurred, being centered at ca. 250 nm, and unlike that seen for **1**, no long wavelength transition was observed. As expected, **Nd.2$_3$** gave transitions with equal magnitude and opposite sign, demonstrating that the two complexes were formed as a structurally identical pair of enantiomers. Parker and coworkers[32] have investigated the use of these same chiral antennae (as well as the 2-isomers) in C_4-symmetry based tetranaphthyl based cyclen ligands and Eu(III) complexes. While the structures are quite different to those presented herein, some similarities exists, which enables us to draw some correlations between our results and that obtained by Parker. Firstly, both results indicate the presence of single chiral stereoisomers in solution for the ligands, and secondly both show the appearance of distinctive bisignate profiles upon formation of the metal ion complexes with

crossover points at 218 nm; which is usually indicative of exciton coupling[33] occurring between the naphthyl chromophores. The CD spectra were also recoded at different temperatures between -10 and +30°C, however, only minor changes were observed in the CD-spectra within this temperature ranges for both systems .

Due to the relatively large changes observed between the free ligands **1** and **2** and their corresponding Nd(III) complexes, we next investigated the formation of the complexes in solution by observing the changes in the CD spectra at room temperature. The overall changes in the circular dichroism spectra of **1** and **2** upon the addition of increasing concentrations of $Nd(CF_3SO_3)_3$ were monitored in CH_3CN at RT and are shown in Figure 4, top and bottom

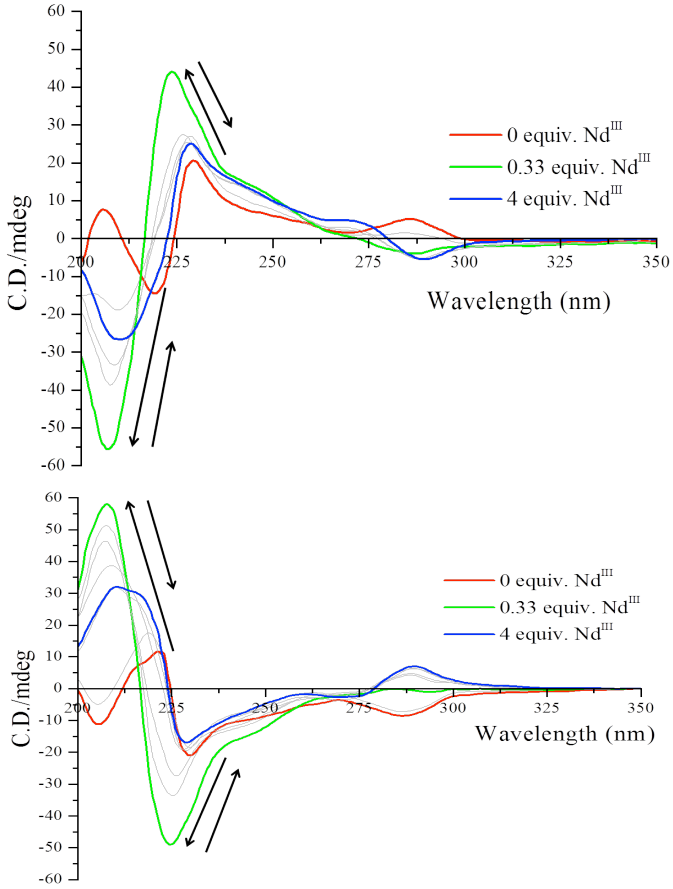

Figure 4. **Top**: The overall changes in the circular dichroism spectrum of **1**, and **bottom**: overall changes in the circular dichroism spectrum of **2** upon titrating against increasing concentrations of $Nd(CF_3SO_3)_3$ (0 – 3 equiv.) at RT in CH_3CN.

respectively. The results demonstrate that significant changes occur upon formation of the Nd(III) directed self-assembly where up to 0.33 equivalents of the metal ion, and the formation of the desired 1:3 (metal:ligand) complex. The aforementioned distinctive bisignate profiles appeared for both; and as above, the two profiles behaved (within experimental error) as previously observed, with equal magnitude and opposite signs, demonstrating that these two self-assemblies are formed in solution as a structurally identical pair of enantiomers. Analyzing the changes observed in Figure 5 further, demonstrates that for **1**, there was an increase in the relative intensity of the positive band located at 229 nm and a shift to 224 nm between the addition of 0→0.33 equivalents of $Nd(CF_3SO_3)_3$. Concurrently, a disappearance in the band centered at 218 nm with the emergence of a negative band at 207 nm was evident within the same concentration range. However, upon additional of Nd(III) between 0.33→ 4 equivalents a decrease was observed in the relative intensities the 207 nm and 224 nm bands which was also accompanied with a shift to 210 and 228 nm, respectively. Importantly, the same trend was also seen for **2**, Figure 4 (bottom). This would indicate that at higher Nd(III) concentrations the 1:3 complex undergoes structural and stoichiometric changes, most likely resulting in the formation of possibly the 1:2 or the 1:1 complexes (which would obviously have different symmetry to that of the desired 1:3 complex) in solution. We have observed similar behavior in related work, where initially the 1:3 stoichiometry is rapidly established (ca. 90% within 0.3 equivalents of the lanthanide ion); followed by the formation of the 1:2 species.[34,35] Hence, the above changes provide an additional handle by which to assess the formation of such chiral self-assembly structures in solution; the formation of which was next examined by observing the changes in the absorption, the ligand centered emission and the metal centered NIR emission.

UV-Visible and luminescence photophysical solution studies of 1 and 2 with $Nd(CF_3SO_3)_3$:

A series of photophysical titrations (absorption and luminescence) were carried out in CH_3CN in order to gain an insight into the stoichiometry of the self-assembly process of **1** and **2** with Nd(III) in solution, and to quantify the binding affinity of the various complexes formed; achieved by fitting the changes observed using non-linear regression analysis (SPECFIT). The

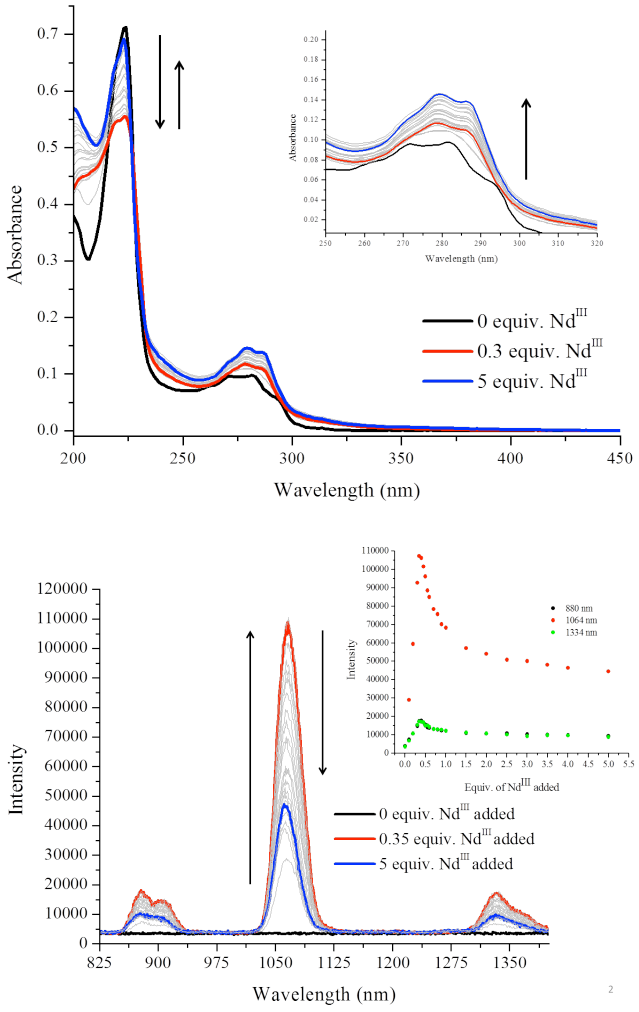

Figure 5. Top: Overall changes in UV-Visible absorption spectra and bottom: overall changes in Nd(III) phosphorescence spectra upon titrating **1** (1 x 10-5 M) against $Nd(CF_3SO_3)_3$ (0 – 5 equiv.) in CH_3CN at room temperature. Upon excitation at 281 nm.

overall changes in the UV-Visible absorption spectrum of **1** upon titrating against $Nd(CF_3SO_3)_3$

are shown in Figure 5. Here, the high energy absorption band centered at 223 nm experienced a hypochromatic effect within the addition of 0→ 0.3 equivalents of the metal salt. As we had anticipated from the CD-results, subsequent addition of Nd(III) then gave rise to a small increase in the absorbance up until the addition of 1 equivalent of Nd(III) after which the absorbance began to plateau. Similarly, the longer wavelength absorption band centered at $\square_{max}$ = 281 nm experienced a sharp increase in absorbance between the additions of 0→1 equivalents of Nd(III); reaching a plateau after the addition of 1 equivalent of metal salt. Identical behavior was observed upon titrating **2** with Nd(III) (See Supporting information Figure S10). These changes are similar to that previously observed in our laboratory.[28] The fluorescence emission was also monitored upon excitation at 281 nm, which was quenched upon addition of Nd(III). But both ligands were not strongly fluorescent and the changes were not analyzed further. In contrast, the emergence of long-lived Nd(III) centered luminescence at long wavelengths was clearly visible, with the appearance of characteristic line-like emission bands 880 nm, 1064 nm and 1334 nm, assigned to the deactivation of the Nd(III) $^4F_{3/2}$ excited state, upon excitation at 281 nm, Figure 5. Here, the NIR emission gradually enhanced between the addition of 0→ 0.35 equivalents of Nd(III) signifying the formation of the 1:3 stoichiometry and at the same time, the occurrence of an efficient energy transfer from the antenna to the Nd(III) center. As was observed in the CD-spectra, significant modulation was also seen above the addition of 0.35 equivalents of Nd(III), indicative of the formation of a new species in solution. The corresponding titration profile where the emission at 880 nm, 1064 nm and 1334 nm was monitored, shown inset in Figure 4, demonstrates this, as after the addition of 0.35 equivalent of Nd(III) the emission intensities sharply decrease, reaching a plateau after the addition of ca. one equivalent of Nd(III). This is

indicative of the evolution of the 1:2, and eventually the lesser emissive 1:1 species in solution as a function of increased Nd(III) concentrations (See also Supporting Information).

These changes observed both in the UV-Vis absorption and the NIR emission were fitted using a nonlinear regression analysis, the fit to the experimental data at three different wavelengths is shown in Figure 6. The speciation distribution diagram obtained form these fits is also shown in Figure 6, showing that upon the addition of 0→ 0.33 equivalents of Nd(III) the predominant species is the 1:3 Nd.**1**$_3$ species, formed in 79% yield, after the addition of 0.33

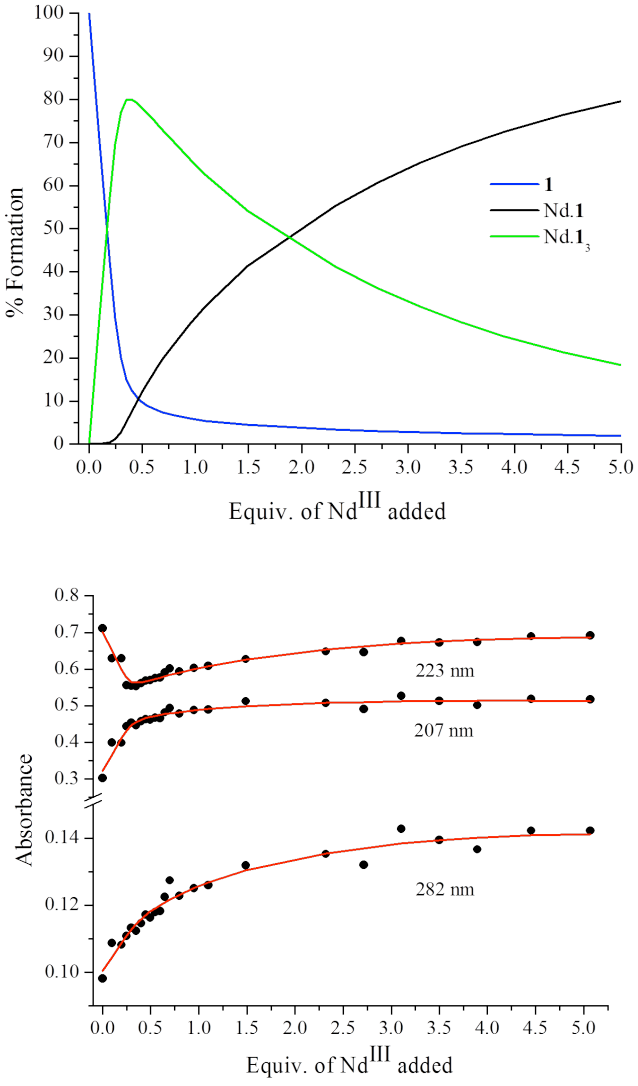

Figure 6. Top: Speciation distribution diagram obtained from UV-Visible absorption titration data fit and bottom: fit of experimental binding isotherms using the non-linear regression analysis program SPECFIT.

equivalents of Nd(III). Additional aliquots of Nd(III) drive the formation of the 1:1 species, Nd.**1**, until it becomes the most dominant species in solution. Nearly identical titration behavior was exhibited by **2**, as shown in supporting information Figure S11-S15. Binding constants and speciation percentage values obtained for the analyses of the UV-Visible titration data are summarized in Table 3; and show that the Nd.$\mathbf{1}_3$ species is formed with a high binding constant

Table 3. Binding constants and speciation distribution percentages values obtained from both UV-visible absorption and luminescence titration data fits for both R and S enantiomers **1** and **2**.

Ligand	UV-visible		Luminescence	
	$\log\beta_{1:1}$	$\log\beta_{1:3}$	$\log\beta_{1:1}$	$\log\beta_{1:3}$
1	6.0 ± 0.3	18.3 ± 0.6	6.2 ± 0.2	17.2 ± 0.4
2	6.1 ± 0.2	17.8 ± 0.4	6.5 ± 0.2	17.8 ±0.3
	% Species at M:L = 1:3		% Species at M:L = 1:3	
1	4	79	12	53
2	8	74	11	67

of $\log\beta_{1:3}$ of 18.3±0.6 for **1** while for **2** a binding constant of 17.8±0.4 was obtained. Interestingly, the formation of the 2:1 species was not observed; an indication that it is short lived, but the 1:1 complex formation gave $\log\beta_{1:1}$ of 6.0±0.3 for **1** while for **2** $\log\beta_{1:1}$ of 6.1±0.2 was obtained. In a similar manner the changes in the lanthanide-centered emission were analyzed (See fits and speciation diagrams in Supporting Information). As for the ground state changes, the titration of both **1** and **2** supported the formation of the 3:1 species in solution within the addition of 0.33 equivalents; with $\log\beta_{1:3}$ of 17.2±0.2 and 17.3±0.8 for **1** and **2**, respectively. These binding constants are comparable to those obtained for other pyridyl amide based self-assembly systems developed in our laboratory.[34] Having established the ability of **1** and **2** to form 3:1 self-assemblies in the presence of Nd(III), we next investigated their self-assembly formation at an air-water interface by forming Langmuir films. Only a small numbers

of examples of lanthanide based Langmuir-Blodgett films, (LB-films) made from the use of thermodynamically and kinetically stable lanthanide complexes have been developed to date,[36,37] and to the best of our knowledge, no examples of NIR emitting LB-films (or NIR luminescent monolayers) have been developed to date[38], but such systems have potential applications in sensing, imaging and telecommunications.

Langmuir monolayer formation: The ability of complexes Nd.**1**$_3$ and Nd.**2**$_3$ to self-assemble at an air-water interface and form Langmuir monolayers was investigated by spreading 20 μL aliquots of each complex (~2.4×10^{-4} M) using $CHCl_3$:CH_3OH (9:1) as the spreading solvent, onto the surface of a water subphase at room temperature. A typical surface pressure-area isotherm was obtained in each case, see Figure 7, in which an exponential increase in surface pressure evidenced the different phase transitions, i.e. gaseous (G), liquid expanded (LE), liquid condensed (LC) and film collapse (C), upon area decrease. The films collapsed at 33 mN m^{-1} for Nd.**1**$_3$ and 32 mN m^{-1} for Nd.**2**$_3$ with areas of 70 ± 5 Å^2 per molecule. The areas of these Nd(III)

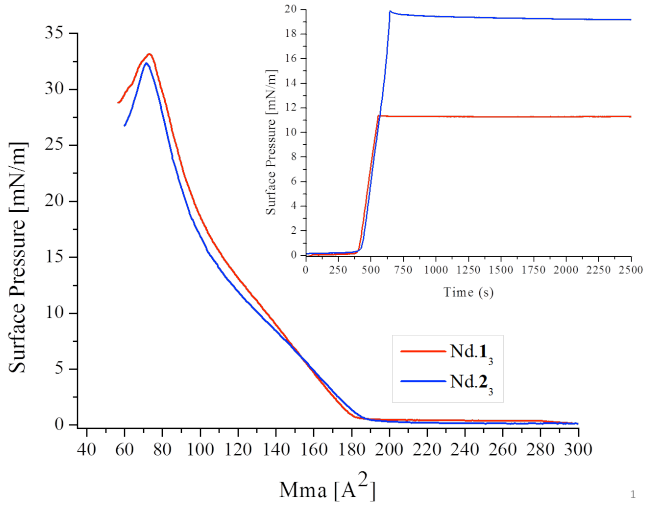

Figure 7. Surface pressure-area isotherm of complexes Nd.**1**$_3$ and Nd.**2**$_3$. Inset: Surface pressure-time stability profiles for Nd.**1**$_3$ and Nd.**2**$_3$.

complexes are approximately those expected for three alkyl chains (ca. 66 $Å^2$ per molecule) and indicate that the complexes remain intact at the air-water interface with supramolecular organization into monolayers, in agreement with our previous results.[28] The Langmuir monolayer stability was also assessed by maintaining the monolayers at the liquid-condensed phase for an extended period of time (exceeding 40 minutes) and monitoring the surface pressure over that same time. The results are shown as inset in Figure 7, demonstrating excellent stability properties for both the Nd.$\mathbf{1}_3$ and the Nd.$\mathbf{2}_3$ films. Each amphiphilic complex was then transferred onto a quartz slide, generating Langmuir-Blodgett films with good quality (smooth) transfer ratios of ~ 1 on the emersion of the quartz slide, demonstrating the successful formation of self-assembly monolayer of Nd.$\mathbf{1}_3$ and Nd.$\mathbf{2}_3$.

Having successfully formed the Langmuir-Blodgett films of Nd.$\mathbf{1}_3$ and Nd.$\mathbf{2}_3$, their photophysical properties were next evaluated. The UV-Visible absorption spectra were recoded and their NIR emission properties were probed by recording Time Resolved Emission Spectra, see Figure 8 and supporting information Figure S16. We were however, unable to obtain reliable CD spectra of these (single monolayer based) Langmuir-Blodgett films. The absorption spectra of the monolayers matched those seen for the complexes in solution, demonstrating that the films existed as the expected 3:1 complexes. More importantly, for both systems, the NIR centered Nd(III) emission was observed from each film upon excitation at 337 nm with bands centered at $\square$ = 880 nm and 1064 nm, representing deactivation from the Nd^{III} $^4F_{3/2}$ excited state to ground states $^4I_{9/2}$, and $^4I_{11/2}$. The weaker $^4F_{3/2} \rightarrow {}^4I_{13/2}$ transition at 1334 nm was not observed due to significant noise in the spectrum arising from scattered light from the fourth harmonic of the excitation pulse. Attempts to remove the signal arising from scatter by using bandpass or interference filters merely resulted in a diminution of the overall signal. However, it is clear from

comparison of the relative intensities of the 880 and 1064 nm peaks in solution and on the surface that the complex symmetry is very similar on both occasions, since the 1064 nm transition is hypersensitive to symmetry (□J = 4). These results are quite significant as they demonstrate that a lanthanide NIR emission can be recoded even from a single monolayer, clearly demonstrating the sensitivity of the system.

The LB films have been found to be stable under ambient conditions over a period of many months. The excited-state decay of the Nd(III) centered emission was also determined for

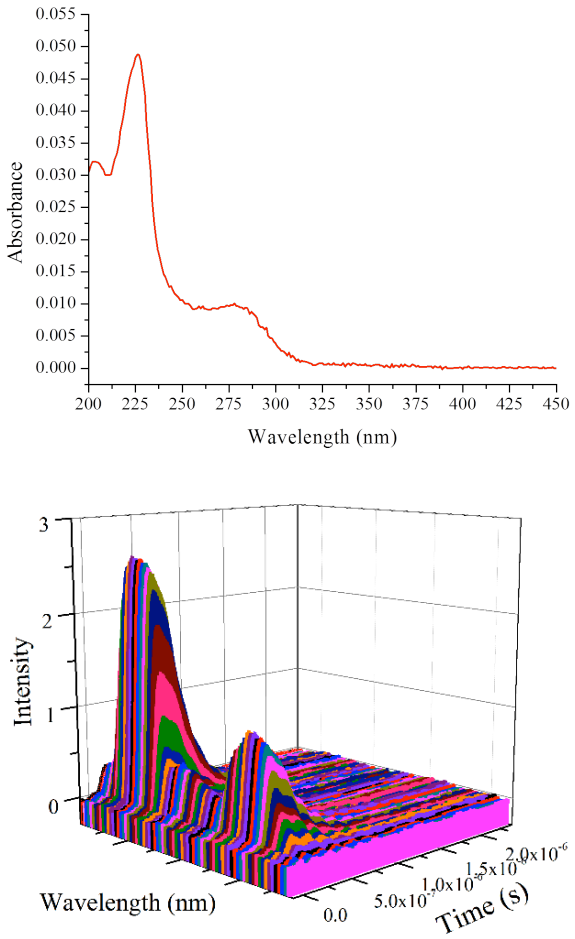

Figure 8. Top: Absorption spectrum of Langmuir-Blodgett Nd.**1**$_3$ monolayer and bottom: Time-resolved emission spectrum of Nd.**1**$_3$ monolayer after excitation at 337 nm, showing sensitized Nd^{III}-based luminescence.

both of these films, and was found to be similar to that observed above in solution (See Supporting Information Table S2). Whilst this paper represents our first steps in this area, we are currently investigating other Ln^{III} containing amphiphilic complexes for these purposes.

Conclusion

We have successfully developed amphiphilic, chiral, Nd(III) systems that form through facile lanthanide directed self-assembly processes. The inclusion of the hexadecyl chain in **1** and **2** leads to the formation of stable and well-formed Langmuir films at an Air-Water interface. Furthermore, the successful transfer of these onto solid supports (quartz slides) gave, for the first time, time delayed NIR centered luminescence which, by comparing to the solution state measurements, was relatively unaltered upon immobilization. Such NIR Immobilized Luminescent Chiral Devices (NIR-ICLDs) have potential application in chiral sensing of biological media as well as in multiple wavelength emissive systems, areas that we are now investing significant time and effort into.

Acknowledgements

We thank the Science Foundation Ireland (SFI), the Irish Research Council for Science, Engineering & Technology (IRCSET) and the European Research Council (ERC) for financial support. We would also like to thank Dr. Nicholas G. White for assistance with X-ray data.

Abbreviations

NIR, near infrared; LB, Langmuir-Blodgett; A-W, Air-Water; LC, Liquid condensed; LE, Liquid expanded; G, Gaseous; C, Collapse; CD, Circular dichroism; CPL, Circularly polarized luminescence.

References

(1) Binnemans, K. *Chem. Rev.* **2009**, *109*, 4283.

(2) Faulkner, S.; Natrajan, L. S.; Perry, W. S.; Sykes, D. *Dalton Trans* **2009**, 3890.

(3) Bunzli, J.-C. G.; Piguet, C. *Chem. Soc. Rev.* **2005**, *34*, 1048.

(4) Lincheneau, C.; Stomeo, F.; Comby, S.; Gunnlaugsson, T. *Aust. J. Chem.* **2011**, *64*, 1315.

(5) Pandya, S.; Yu, J.; Parker, D. *Dalton Trans.* **2006**, 2757.

(6) Eliseeva, S. V.; Bunzli, J.-C. G. *Chem. Soc. Rev.* **2009**, *39*, 189.

(7) Bunzli, J.-C. G. *Chem. Rev.* **2010**, *110*, 2729.

(8) dos Santos, C. M. G.; Harte, A. J.; Quinn, S. J.; Gunnlaugsson, T. *Coordin. Chem. Rev.* **2008**, *252*, 2512.

(9) Ward, M. D. *Coordin. Chem. Rev.* **2010**, *254*, 2634.

(10) Faulkner, S.; Pope, S. J. A.; Burton-Pye, B. P. *Appl Spec Rev* **2005**, *40*, 1.

(11) Aboshyan-Sorgho, L.; Besnard, C.; Pattison, P.; Kittilstved, K. R.; Aebischer, A.; Bunzli, J.-C. G.; Hauser, A.; Piguet, C. *Angew. Chem. Int. Ed.* **2011**, *50*, 4108

(12) Beeby, A.; Burton-Pye, B. P.; Faulkner, S.; Motson, G. R.; Jeffery, J. C.; McCleverty, J. A.; Ward, M. D. *Dalton Trans* **2002**, 1923.

(13) Beeby, A.; Faulkner, S. *Chem Phys Lett* **1997**, *266*, 116.

(14) Beeby, A.; Faulkner, S.; Parker, D.; Williams, J. A. G. *J. Chem. Soc. Perkin Trans. 2* **2001**, 1268.

(15) Faulkner, S.; Beeby, A.; Carrie, M.-C.; Dadabhoy, A.; Kenwright, A. M.; Sammes, P. G. *Inorg Chem Comm* **2001**, *4*, 187.

(16) Wada, Y.; Okubo, T.; Ryo, M.; Nakazawa, T.; Hasegawa, Y.; Yanagida, S. *J. Am. Chem. Soc.* **2000**, *122*, 8583.

(17) Yanagida, S.; Hasegawa, Y.; Murakoshi, K.; Wada, Y.; Nakashima, N.; Yamanaka, T. *Coordin. Chem. Rev.* **1998**, 461.

(18) Pope, S. J. A.; Coe, B. J.; Faulkner, S.; Bichenkova, E. V.; Yu, X.; Douglas, K. T. *J. Am. Chem. Soc.* **2004**, *126*, 9490.

(19) Perry, W. S.; Pope, S. J. A.; Allain, C.; Coe, B. J.; Kenwright, A. M.; Faulkner, S. *Dalton Trans.* **2010**, *39*, 10974.

(20) Nonat, A. M.; Allain, C. M.; Faulkner, S.; Gunnlaugsson, T. *Inorg. Chem.* **2010**, *49*, 8449.

(21) Faulkner, S.; Carrié, M.-C.; Pope, S. J. A.; Squire, J.; Beeby, A.; Sammes, P. G. *Dalton Trans.* **2004**, 1405.

(22) Truman, L. K.; Comby, S.; Gunnlaugsson, T. *Angew. Chem. Int. Edit.* **2012**, *51*, 9624

(23) Gunnlaugsson, T.; McCoy, C. P.; Stomeo, F. *Tetrahedron Lett*. **2004**, *45*, 8403.

(24) Stomeo, F.; Plush, S. E.; Gunnlaugsson, T. *Chem. Mater*. **2006**, *18*, 4336.

(25) Massue, J.; Quinn, S. J.; Gunnlaugsson, T. *J. Am. Chem. Soc*. **2008**, *130*, 6900.

(26) Bonnet, C. S.; Massue, J.; Quinn, S. J.; Gunnlaugsson, T. *Org. Biomol. Chem.,* **2009**, 3074.

(27) Murray, N. S.; Jarvis, S. P.; Gunnlaugsson, T. *Chem. Commum*. **2009**, 4959.

(28) Kitchen, J. A.; Barry, D. E.; Mercs, L.; Albrecht, M.; Peacock, R. D.; Gunnlaugsson, T. *Angew. Chem. Int. Ed* **2011**, *51*, 704

(29) Cosier, J.; Glazer, A. M. *J. Appl. Cryst*. **1986**, *19*, 105.

(30) Otwinowski, Z.; Minor, W. *Processing of X-ray Diffraction Data Collected in Oscillation Mode, Methods Enzymol* **1997** *276*.

(31) Sheldrick, G. M. *Acts Crystallogr., Sect. A*. **2008**, *A64*, 112.

(32) Dickens, R. S.; Howard, J. A. K.; Maupin, C. L.; Maloney, J. M.; Parker, D.; Peacock, R. D.; Riehl, J. P.; Siligard, G. *New J. Chem*, **1998**, 891.

(33) Satrijo, A.; Meskers, S. C. J.; Swager, T. M. *J. Am. Chem. Soc*. **2006**, *128*, 9030.

(34) Lincheneau, C.; Destribats, C.; Barry, D. E.; Kitchen, J. A.; Peacock, R. D.; Gunnlaugsson, T. *Dalton Trans*., **2011**, *40*, 12056.

(35) We have also seen such effect in double stranded dimetallic helicate formations: Stomeo, F.; Lincheneau, C.; Leonard, J. P.; O'Brien, J. E.; Peacock, R. D.; McCoy, C. P.; Gunnlaugsson, T. *J. Am. Chem. Soc.,* **2009**, *131*, 9636.

(36)

(37)

(38) Matsumoto and co-workers have recently shown that NIR emissive lanthanide doped nanoparticles can be dip-coded onto plastic sheets: Watanabe, S.; Hyodo, H.; Taguchi, H.; Soga, K.; Takanashi, Y.; Matsumoto, M. *J. Oleo Sci*. **2012**, *61*, 565-573.